The Physics and Cosmology of TeV Blazars

Christoph Pfrommer[1]

in collaboration with

Avery E. Broderick[2], Phil Chang[3], Ewald Puchwein[1], Volker Springel[1]

[1]Heidelberg Institute for Theoretical Studies, Germany
[2]Perimeter Institute/University of Waterloo, Canada
[3]University of Wisconsin-Milwaukee, USA

Jul 11, 2012 / Meeting, DFG Research Unit FOR 1254

The Hitchhiker's Guide to . . . Blazar Heating

- the extragalactic TeV Universe
- plasma physics for cosmologists
- consequences for
  - intergalactic magnetic fields
  - extragalactic gamma-ray background
  - thermal history of the Universe
  - Lyman-α forest
  - “missing dwarf galaxies”
  - H I mass function
  - galaxy cluster bimodality

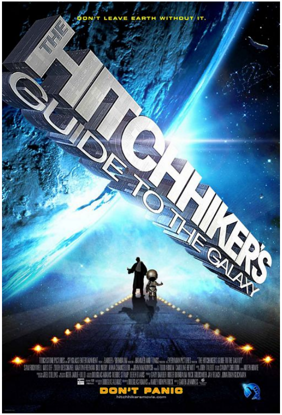

TeV gamma-ray astronomy

H.E.S.S.

MAGIC I

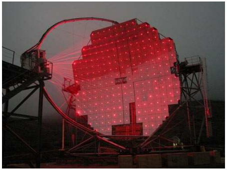

VERITAS

MAGIC II

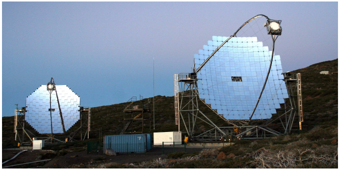

The TeV gamma-ray sky

There are several classes of TeV sources:

- Galactic - pulsars, BH binaries, supernova remnants
- Extragalactic - **mostly** blazars, two starburst galaxies

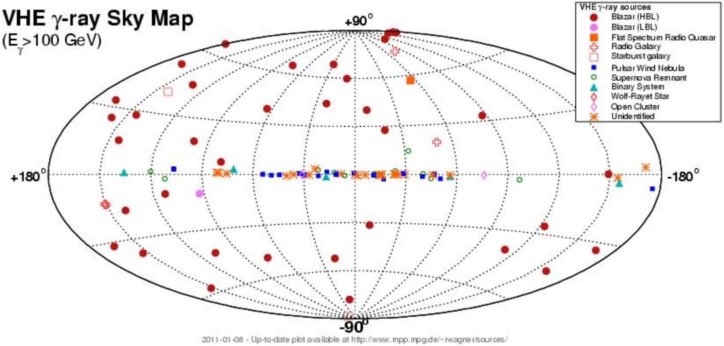

Unified model of active galactic nuclei

narrow line region

broad line region

dusty torus

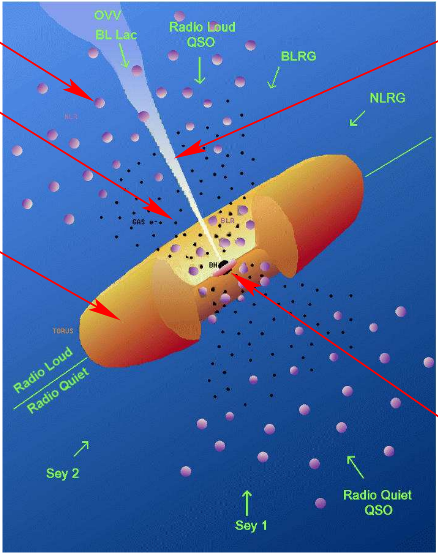

relativistic jet

central SMBH

The blazar sequence

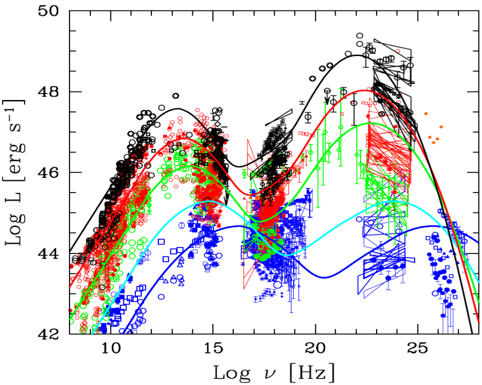

Ghisellini (2011), arXiv:1104.0006

- continuous sequence from LBL–IBL–HBL
- TeV blazars are dim (very sub-Eddington)
- TeV blazars have rising spectra in the Fermi band ($\alpha < 2$)
- define TeV blazar = hard IBL + HBL

Propagation of TeV photons

- 1 TeV photons can pair produce with 1 eV EBL photons:

$$\gamma_{\mathrm{TeV}} + \gamma_{\mathrm{eV}} \rightarrow e^+ + e^-$$

- mean free path for this depends on the density of 1 eV photons:
  $\rightarrow \lambda_{\gamma\gamma} \sim (35 \ldots 700)$ Mpc for $z = 1 \ldots 0$
  $\rightarrow$ pairs produced with energy of 0.5 TeV ($\gamma = 10^6$)
- these pairs inverse Compton scatter off the CMB photons:
  $\rightarrow$ mean free path is $\lambda_{\mathrm{IC}} \sim \lambda_{\gamma\gamma}/1000$
  $\rightarrow$ producing gamma-rays of $\sim$ 1 GeV

$$E \sim \gamma^2 E_{\mathrm{CMB}} \sim 1\ \mathrm{GeV}$$

- each TeV point source should also be a GeV point source

What about the cascade emission?

Every TeV source should be associated with a 1-100 GeV gamma-ray halo – **not seen!**

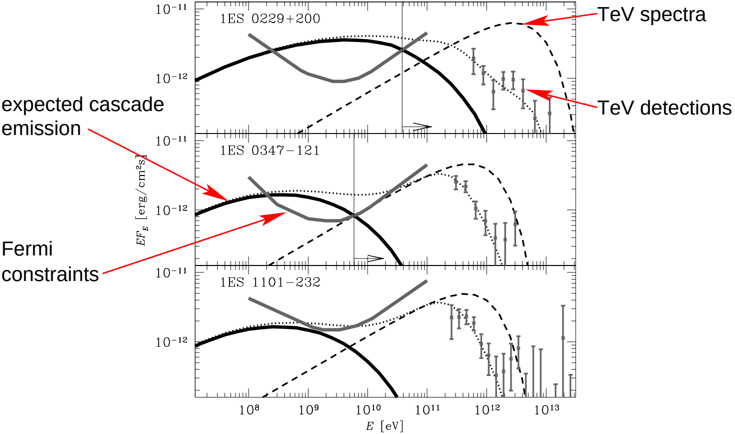

Neronov & Vovk (2010)

Measuring IGM *B*-fields from TeV/GeV observations

- TeV beam of e^+/e^- are deflected out of the line of sight reducing the GeV IC flux → lower limit on B
- Larmor radius

$$r_\mathrm{L} = \frac{E}{eB} \sim 30 \left(\frac{E}{3\,\mathrm{TeV}}\right) \left(\frac{B}{10^{-16}\,\mathrm{G}}\right)^{-1} \mathrm{Mpc}$$

- IC mean free path

$$x_\mathrm{IC} \sim 0.1 \left(\frac{E}{3\,\mathrm{TeV}}\right)^{-1} \mathrm{Mpc}$$

- for the associated 10 GeV IC photons the *Fermi* angular resolution is 0.2° or $\theta \sim 3 \times 10^{-3}$ rad

$$\frac{x_\mathrm{IC}}{r_\mathrm{L}} > \theta \to B \gtrsim 10^{-16}\,\mathrm{G}$$

Missing plasma physics?

How do beams of e^+/e^- propagate through the IGM?

- plasma processes are important
- interpenetrating beams of charged particles are unstable
- consider the two-stream instability:

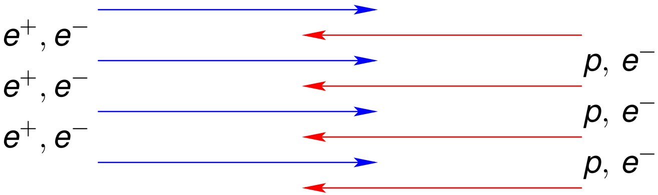

- one frequency (timescale) and one length in the problem:

$$\frac{\omega_p}{\gamma} = \sqrt{\frac{4\pi e^2 n_e}{\gamma^2 m_e}}, \qquad \lambda_p = \frac{\gamma c}{\omega_p} \sim 10^{14}\,\mathrm{cm} \times \left(\frac{\gamma}{10^6}\right)\Big|_{\bar{\rho}(z=0)}$$

Two-stream instability: mechanism

wave-like perturbation with $\boldsymbol{k} || \boldsymbol{v}_{\text{beam}}$, longitudinal charge oscillations in background plasma (Langmuir wave):

- initially homogeneous beam-e^-:
  attractive (repulsive) force by potential maxima (minima)
- e^- attain lowest velocity in potential minima $\rightarrow$ bunching up
- e^+ attain lowest velocity in potential maxima $\rightarrow$ bunching up

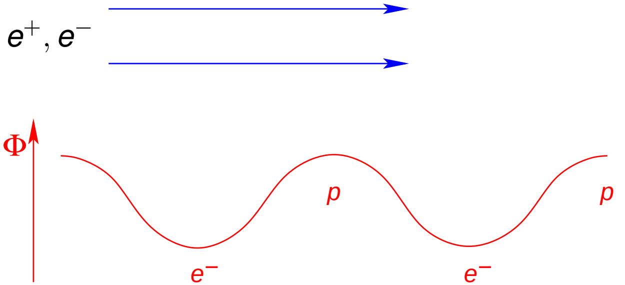

Two-stream instability: mechanism

wave-like perturbation with $\boldsymbol{k} || \boldsymbol{v}_{\text{beam}}$, longitudinal charge oscillations in background plasma (Langmuir wave):

- beam-e^+/e^- couple in phase with the background perturbation: enhances background potential
- stronger forces on beam-e^+/e^- $\rightarrow$ positive feedback
- exponential wave-growth $\rightarrow$ instability

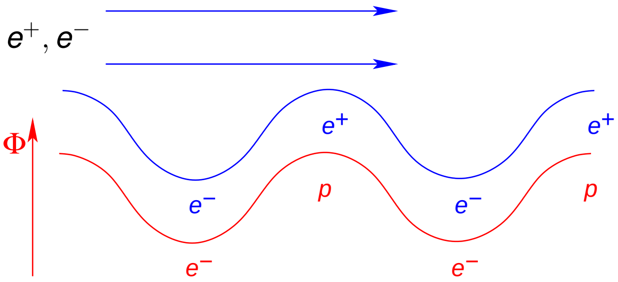

Two-stream instability: energy transfer

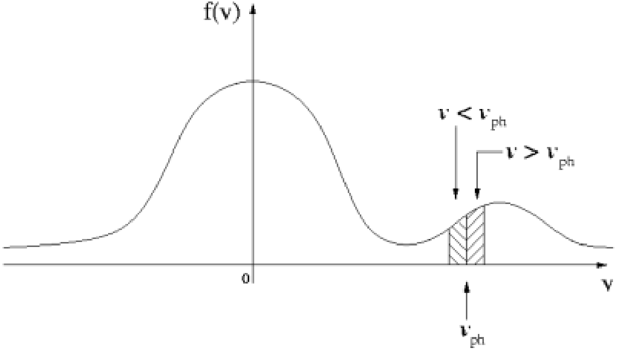

- particles with $v \gtrsim v_{\rm phase}$:
  pair energy → plasma waves → growing modes
- particles with $v \lesssim v_{\rm phase}$:
  plasma wave energy → pairs → damped modes

Oblique instability

k oblique to $\boldsymbol{v}_{\rm beam}$: real word perturbations don't choose "easy" alignment $= \sum$ all orientations

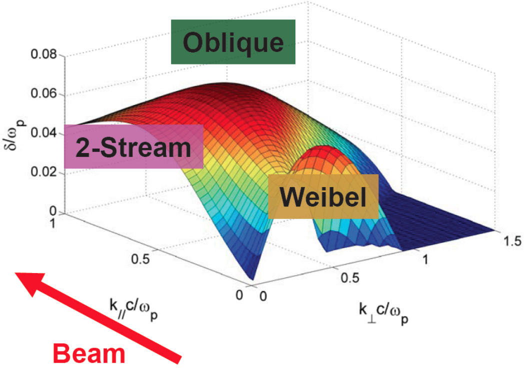

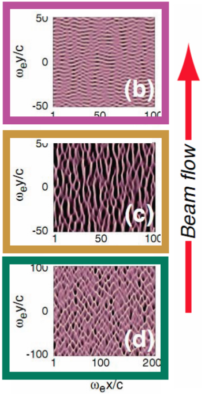

Bret (2009), Bret+ (2010)

Beam physics – growth rates

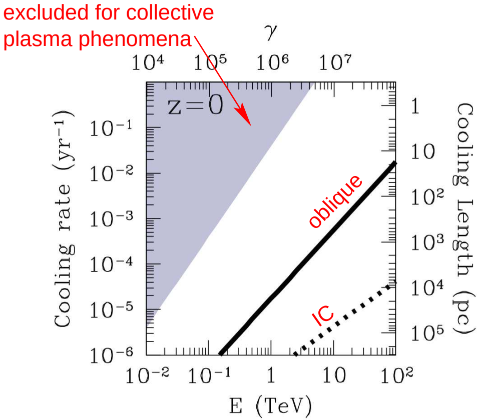

Broderick, Chang, C.P. (2012)

- consider a light beam penetrating into relatively dense plasma
- maximum growth rate

$$\sim 0.4\,\gamma\,\frac{n_{\mathrm{beam}}}{n_{\mathrm{IGM}}}\,\omega_p$$

- oblique instability beats IC by two orders of magnitude

Beam physics – complications . . .

non-linear saturation:

- non-linear evolution of these instabilities at these density contrasts is not known
- expectation from PIC simulations suggest substantial isotropization of the beam
- **assume** that they grow at linear rate up to saturation

→ plasma instabilities dissipate the beam's energy, no (little) energy left over for inverse Compton scattering off the CMB

TeV emission from blazars – a new paradigm

$$\gamma_{\text{TeV}} + \gamma_{\text{eV}} \;\rightarrow\; e^+ + e^- \;\rightarrow\; \begin{cases} \text{IC off CMB} & \rightarrow \quad \gamma_{\text{GeV}} \\ \text{plasma instabilities} & \rightarrow \quad \text{heating IGM} \end{cases}$$

absence of γ_{GeV}'s has significant implications for ...

- intergalactic B-field estimates
- γ-ray emission from blazars: spectra, background

additional IGM heating has significant implications for ...

- thermal history of the IGM: Lyman-α forest
- late time structure formation: dwarfs, galaxy clusters

Implications for *B*-field measurements

Fraction of the pair energy lost to inverse-Compton on the CMB: $f_{IC} = \Gamma_{IC}/(\Gamma_{IC} + \Gamma_{oblique})$

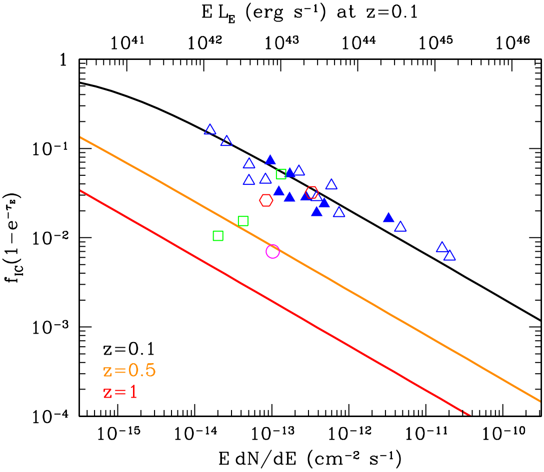

Broderick, Chang, C.P. (2012)

Conclusions on *B*-field constraints from blazar spectra

- it is thought that TeV blazar spectra might constrain IGM *B*-fields
- this assumes that cooling mechanism is IC off the CMB + deflection from magnetic fields
- beam instabilities may allow high-energy e^+/e^- pairs to self scatter and/or lose energy
- isotropizes the beam – no need for *B*-field
- $\lesssim$ 1–10% of beam energy to IC CMB photons

$\rightarrow$ **TeV blazar spectra are not suitable to measure IGM *B*-fields!**

TeV blazar luminosity density: today

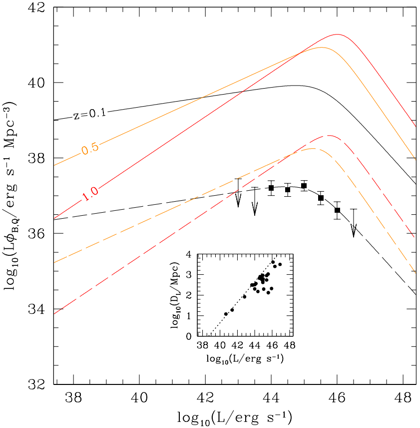

Broderick, Chang, C.P. (2012)

- collect luminosity of all 23 TeV blazars with good spectral measurements
- account for the selection effects (sky coverage, duty cycle, galactic occultation, TeV flux limit)
- TeV blazar luminosity density is a scaled version ($\eta_B \sim 0.2\%$) of that of quasars!

Unified TeV blazar-quasar model

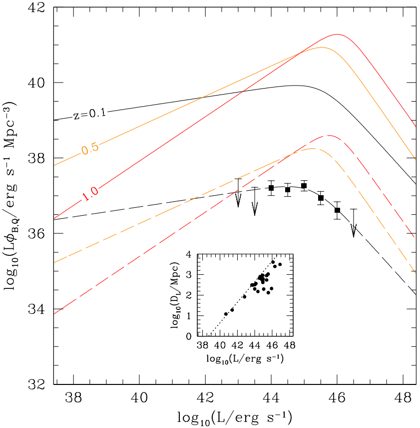

Broderick, Chang, C.P. (2012)

Quasars and TeV blazars are:

- regulated by the same mechanism
- contemporaneous elements of a single AGN population: TeV-blazar activity does not lag quasar activity

→ **assume that they trace each other for all redshifts!**

How many TeV blazars are there?

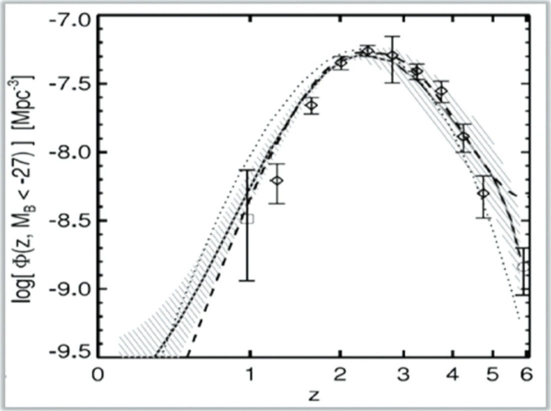

Hopkins+ (2007)

How many TeV blazars are there?

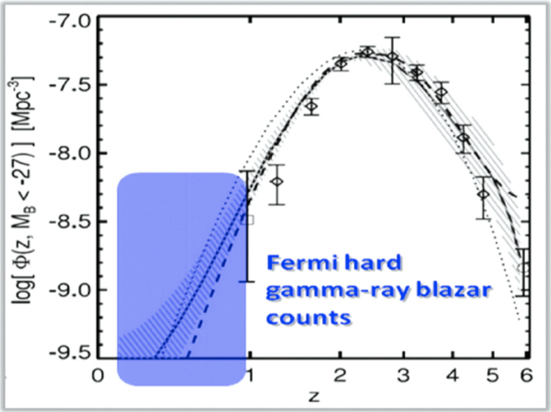

Hopkins+ (2007)

How many TeV blazars are there?

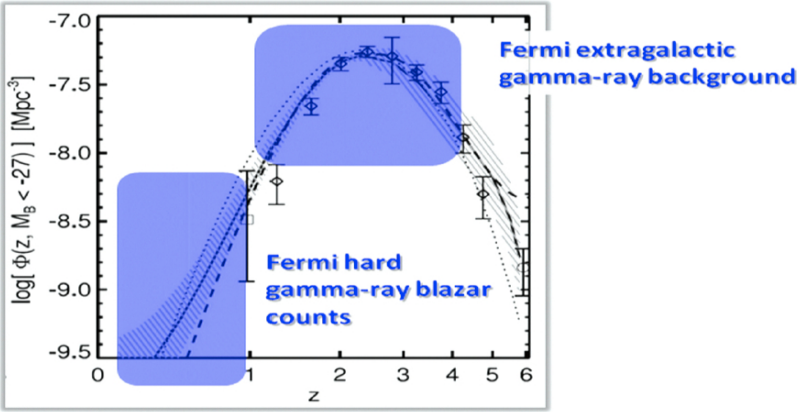

Hopkins+ (2007)

Fermi number count of “TeV blazars”

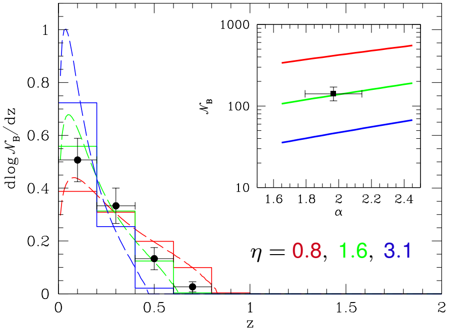

Broderick, Chang, C.P. (2012)

- number evolution of TeV blazars that are expected to have been observed by *Fermi* vs. observed evolution
- colors: different flux (luminosity) limits connecting the *Fermi* and the TeV band:

$$L_{\mathrm{TeV,min}}(z) = \eta\, L_{\mathrm{Fermi,min}}(z)$$

→ evolving (increasing) blazar population consistent with observed declining evolution (*Fermi* flux limit)!

How many TeV blazars are there at high-z?

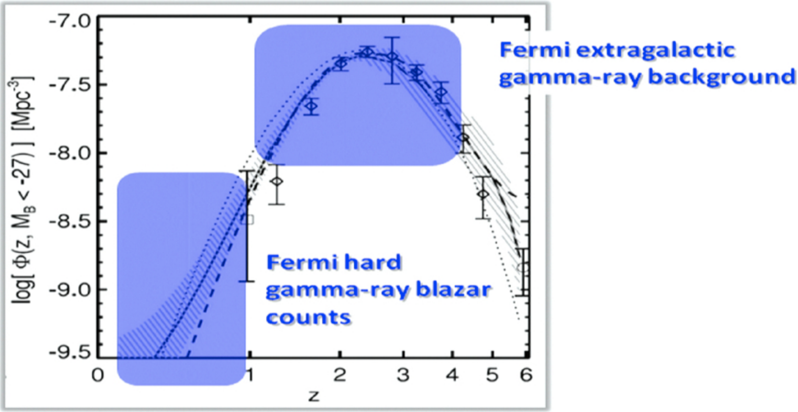

Hopkins+ (2007)

Fermi probes “dragons” of the gamma-ray sky

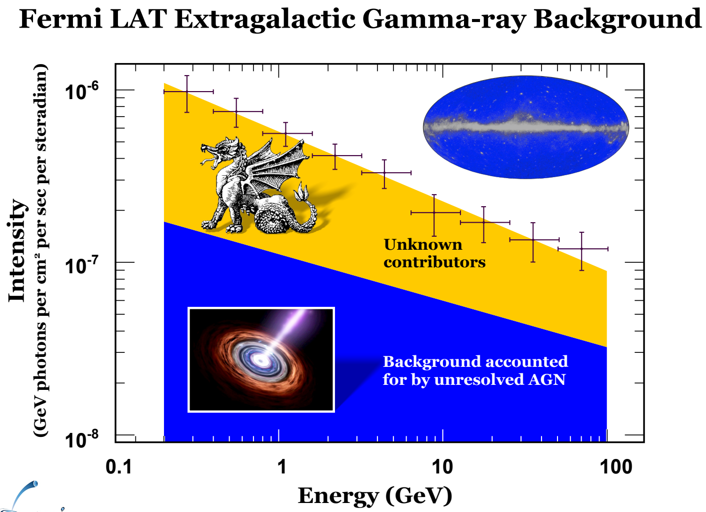

Extragalactic gamma-ray background

- assume all TeV blazars have identical intrinsic spectra:

$$F_E = L\hat{F}_E \propto \frac{1}{(E/E_b)^{\alpha_L - 1} + (E/E_b)^{\alpha - 1}},$$

E_b is break energy,

$\alpha_L < \alpha$ are low and high-energy spectral indexes

- extragalactic gamma-ray background (EGRB):

$$E^2 \frac{dN}{dE}(E,z) = \frac{1}{4\pi} \int_z^\infty dV(z') \frac{\eta_B \tilde{\Lambda}_Q(z') \hat{F}_{E'}}{4\pi D_L^2} e^{-\tau_E(E',z')},$$

$E' = E(1+z')$ is gamma-ray energy at *emission*,
$\tilde{\Lambda}_Q$ is physical quasar luminosity density,

$\eta_B \sim 0.2\%$ is blazar fraction, τ is optical depth

Extragalactic gamma-ray background

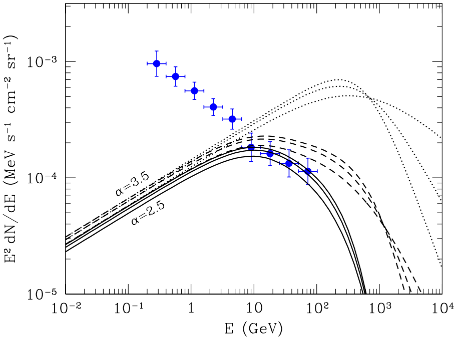

Broderick, Chang, C.P. (2012)

- *dotted:* unabsorbed EGRB due to TeV blazars
- *dashed:* absorbed EGRB due to TeV blazars
- *solid:* absorbed EGRB, after subtracting the resolved TeV blazars ($z < 0.25$)

Evolution of the heating rates

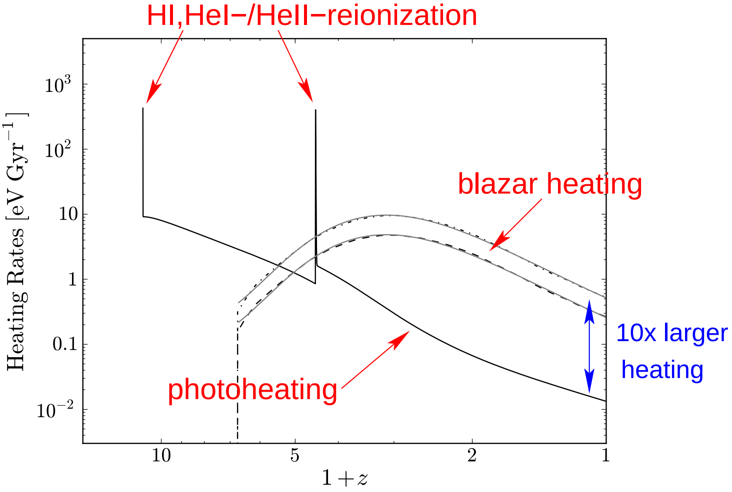

Chang, Broderick, C.P. (2012)

Blazar heating vs. photoheating

- total power from AGN/stars vastly exceeds the TeV power of blazars
- $T_{\rm IGM} \sim 10^4$ K (1 eV) at mean density ($z \sim 2$)

$$\varepsilon_{\rm th} = \frac{kT}{m_{\rm p} c^2} \sim 10^{-9}$$

- radiative energy ratio emitted by BHs in the Universe (Fukugita & Peebles 2004)

$$\varepsilon_{\rm rad} = \eta\,\Omega_{\rm bh} \sim 0.1 \times 10^{-4} \sim 10^{-5}$$

- fraction of the energy energetic enough to ionize H I is ~ 0.1:

$$\varepsilon_{\rm UV} \sim 0.1 \varepsilon_{\rm rad} \sim 10^{-6} \quad \rightarrow \quad kT \sim \text{keV}$$

- photoheating efficiency $\eta_{\rm ph} \sim 10^{-3} \quad \rightarrow \quad kT \sim \eta_{\rm ph}\, \varepsilon_{\rm UV}\, m_{\rm p} c^2 \sim \text{eV}$
  (limited by the abundance of H I/He II due to the small recombination rate)
- blazar heating efficiency $\eta_{\rm bh} \sim 10^{-3} \quad \rightarrow \quad kT \sim \eta_{\rm bh}\, \varepsilon_{\rm rad}\, m_{\rm p} c^2 \sim 10\,\text{eV}$
  (limited by the total power of TeV sources)

Thermal history of the IGM

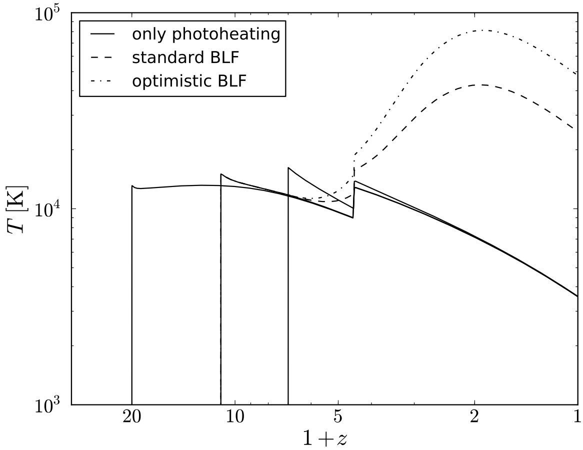

Chang, Broderick, C.P. (2012)

Evolution of the temperature-density relation

no blazar heating

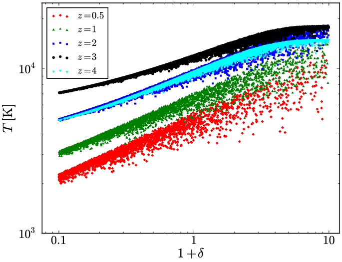

with blazar heating

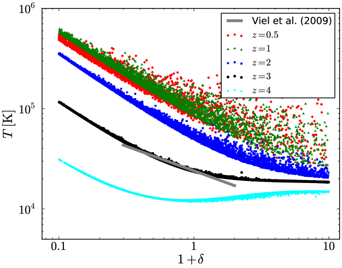

Chang, Broderick, C.P. (2012)

- blazars and extragalactic background light are uniform:
  $\rightarrow$ blazar heating rate independent of density
  $\rightarrow$ makes low density regions *hot*
  $\rightarrow$ causes inverted temperature-density relation, $T \propto 1/\delta$

Blazars cause hot voids

no blazar heating

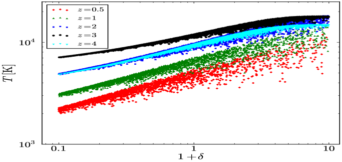

with blazar heating

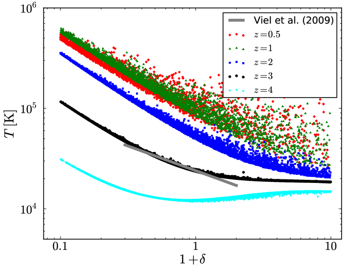

Chang, Broderick, C.P. (2012)

- blazars completely change the thermal history of the diffuse IGM and late-time structure formation

Simulations with blazar heating

Puchwein, C.P., Springel, Broderick, Chang (2012):

- $L = 15h^{-1}\mathrm{Mpc}$ boxes with 2×384^3 particles
- one reference run without blazar heating
- three with blazar heating at different levels of efficiency (address uncertainty)
- used an up-to-date model of the UV background (Faucher-Giguère+ 2009)

Temperature-density relation

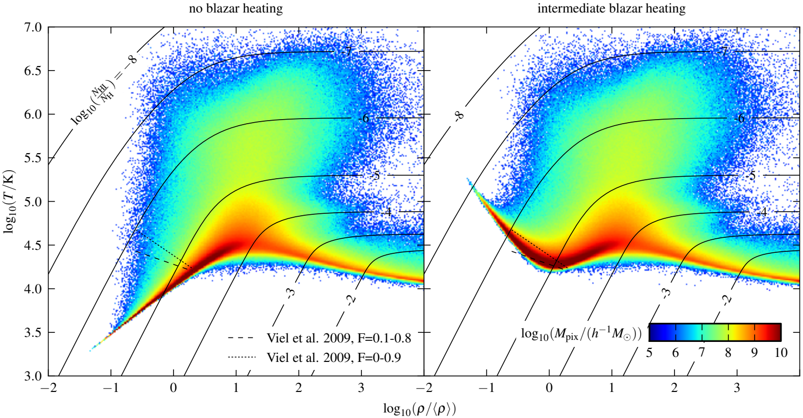

Puchwein, C.P., Springel, Broderick, Chang (2012)

Ly-α spectra

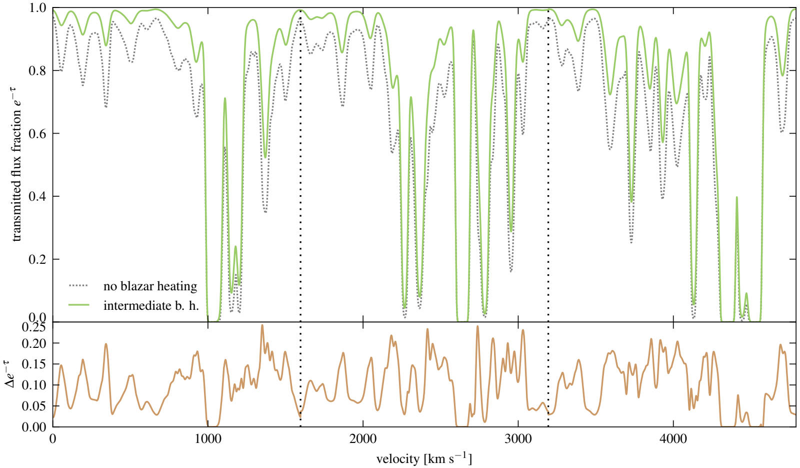

Puchwein+ (2012)

Optical depths and temperatures

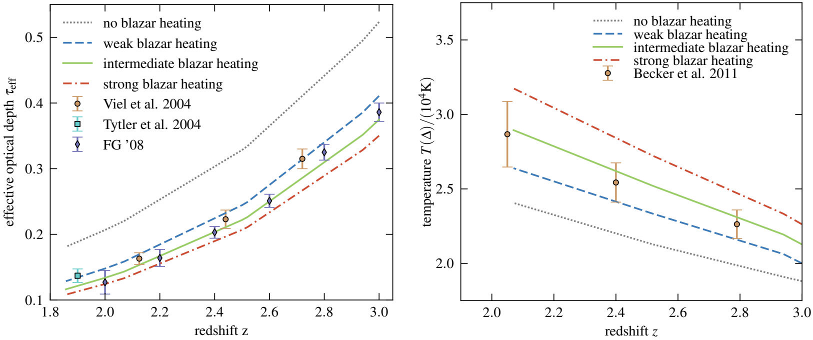

Puchwein+ (2012)

Redshift evolutions of effective optical depth and IGM temperature match data only with additional heating, e.g., provided by blazars!

Ly-α flux PDFs and power spectra

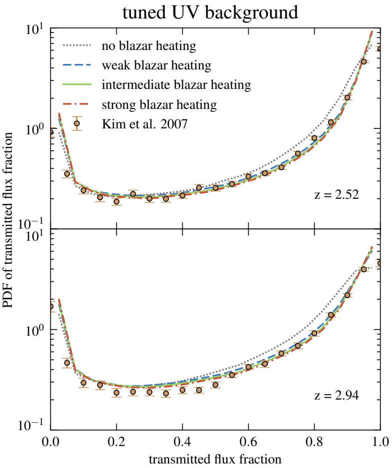

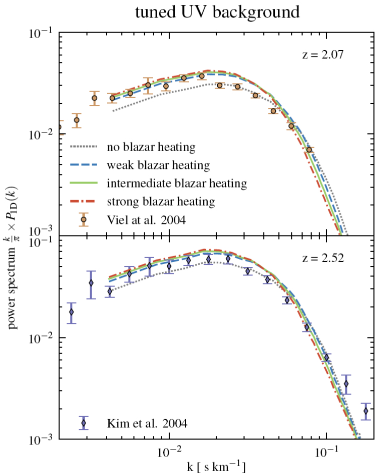

Puchwein+ (2012)

Voigt profile decomposition

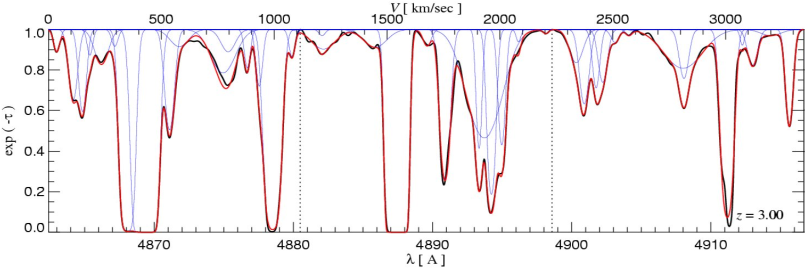

- decomposing Lyman-α forest into individual Voigt profiles
- allows studying the thermal broadening of absorption lines

Voigt profile decomposition – line width distribution

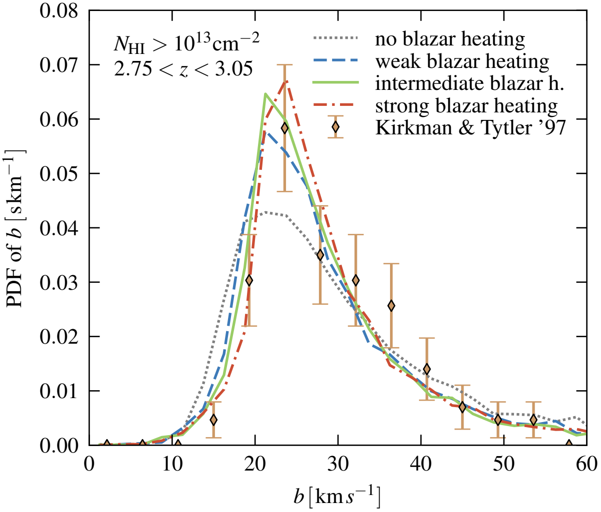

Puchwein+ (2012)

Lyman-α forest in a blazar heated Universe

improvement in modelling the Lyman-α forest is a direct consequence of the peculiar properties of blazar heating:

- heating rate independent of IGM density $\rightarrow$ naturally produces the inverted T–ρ relation that Lyman-α forest data demand
- recent and continuous nature of the heating needed to match the redshift evolutions of all Lyman-α forest statistics
- magnitude of the heating rate required by Lyman-α forest data $\sim$ the total energy output of TeV blazars (or equivalently $\sim$ 0.2% of that of quasars)

Entropy evolution

temperature evolution

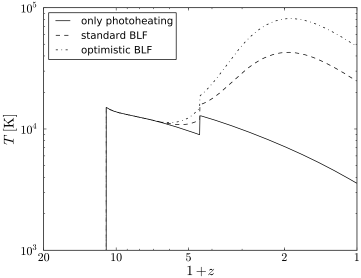

entropy evolution

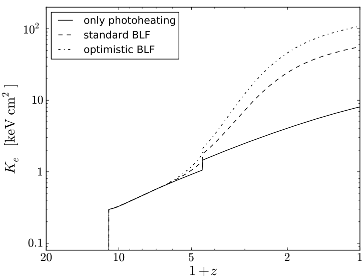

C.P., Chang, Broderick (2012)

- evolution of entropy, $K_e = kTn_e^{-2/3}$, governs structure formation
- blazar heating: late-time, evolving, modest entropy floor

Dwarf galaxy formation – Jeans mass

- thermal pressure opposes gravitational collapse on small scales
- characteristic length/mass scale below which objects do not form
- hotter IGM $\rightarrow$ higher IGM pressure $\rightarrow$ higher Jeans mass:

$$M_J \propto \frac{c_s^3}{\rho^{1/2}} \propto \left(\frac{T_{\mathrm{IGM}}^3}{\rho}\right)^{1/2} \quad \rightarrow \quad \frac{M_{J,\mathrm{blazar}}}{M_{J,\mathrm{photo}}} \approx \left(\frac{T_{\mathrm{blazar}}}{T_{\mathrm{photo}}}\right)^{3/2} \gtrsim 30$$

$\rightarrow$ depends on instantaneous value of c_s

- "filtering mass" depends on full thermal history of the gas: accounts for delayed response of pressure in counteracting gravitational collapse in the expanding universe
- apply corrections for non-linear collapse

Dwarf galaxy formation – Filtering mass

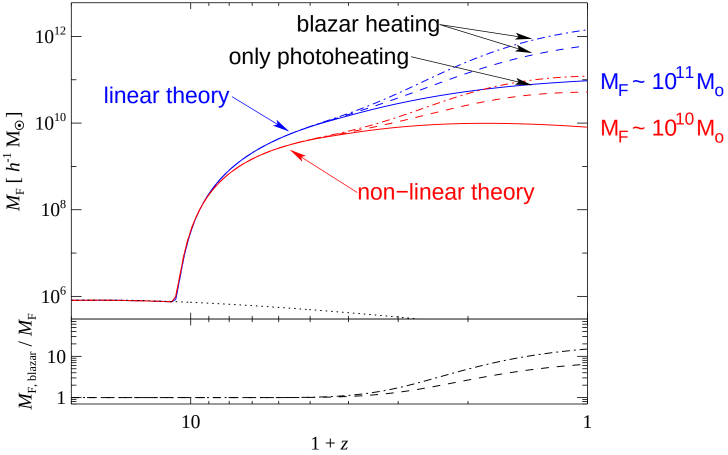

C.P., Chang, Broderick (2012)

Peebles' void phenomenon explained?

mean density | void, $1 + \delta = 0.5$

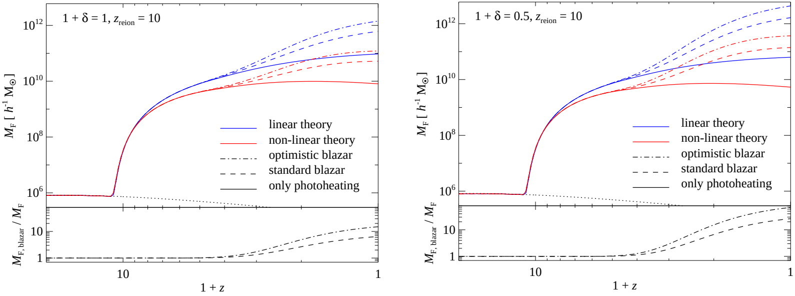

C.P., Chang, Broderick (2012)

- blazar heating efficiently suppresses the formation of void dwarfs within existing DM halos of masses $< 3 \times 10^{11}\ M_\odot$ $(z = 0)$
- may reconcile the number of void dwarfs in simulations and the paucity of those in observations

HITS

“Missing satellite” problem in the Milky Way

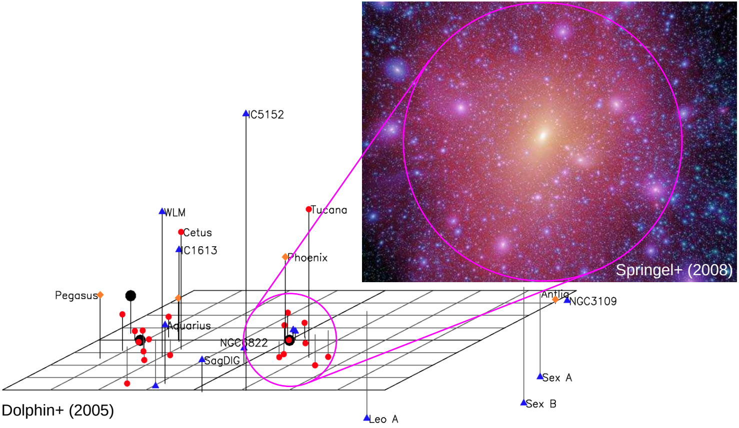

Dolphin+ (2005)

Substructures in cold DM simulations much more numerous than observed number of Milky Way satellites!

When do dwarfs form?

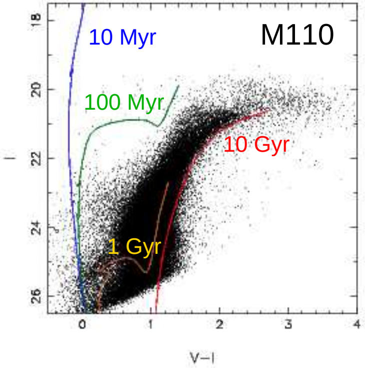

Dolphin+ (2005)

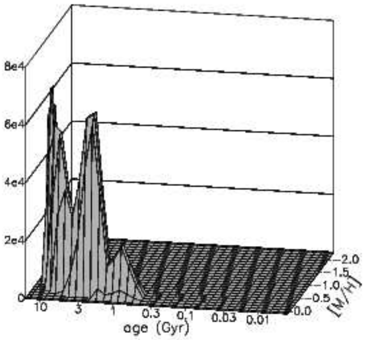

isochrone fitting for different metallicities → star formation histories

When do dwarfs form?

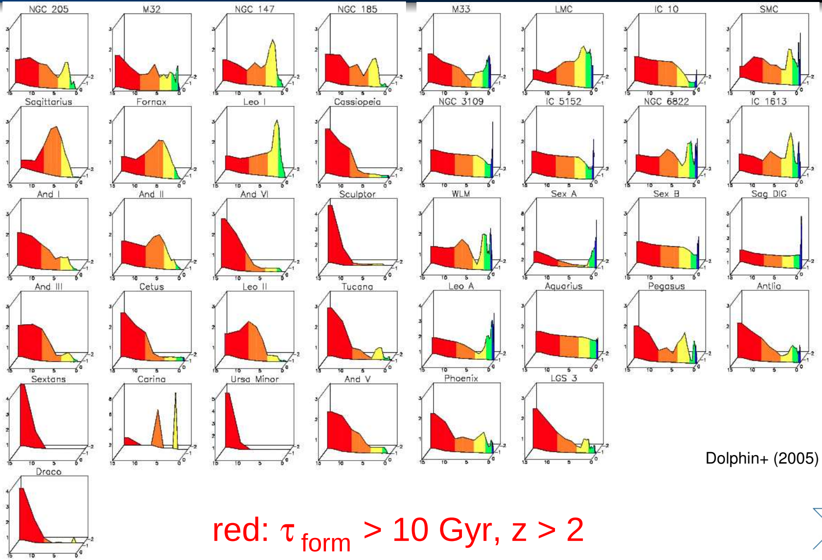

Dolphin+ (2005)

red: $\tau_{\rm form} > 10$ Gyr, $z > 2$

Milky Way satellites: formation history and abundance

satellite formation time

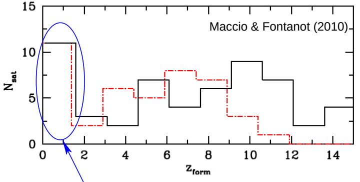

satellite luminosity function

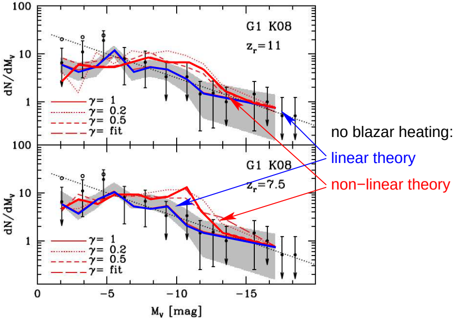

Maccio+ (2010)

- blazar heating suppresses late satellite formation, may reconcile low observed dwarf abundances with CDM simulations

Galactic H I-mass function

Mo+ (2005)

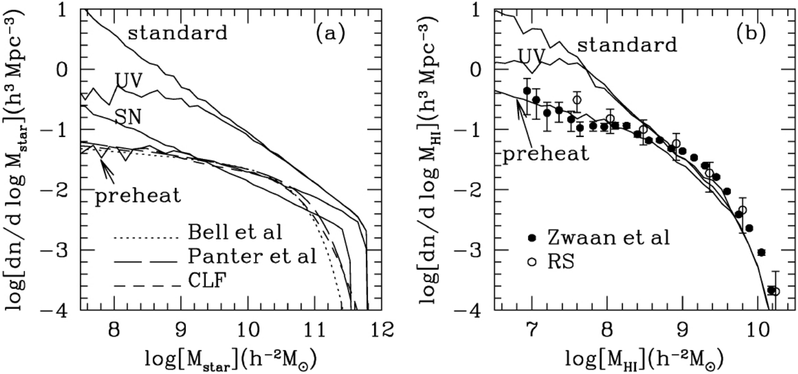

- H I-mass function is too flat (i.e., gas version of missing dwarf problem!)
- photoheating and SN feedback too inefficient
- IGM entropy floor of $K \sim 15\,\mathrm{keV\,cm}^2$ at $z \sim 2-3$ successful!

Conclusions on blazar heating

- explains puzzles in high-energy astrophysics:
  - lack of GeV bumps in blazar spectra without IGM B-fields
  - *unified TeV blazar-quasar model* explains Fermi source counts and extragalactic gamma-ray background
- novel mechanism; dramatically alters thermal history of the IGM:
  - uniform and z-dependent preheating
  - rate independent of density $\rightarrow$ inverted T–ρ relation
  - quantitative self-consistent picture of high-z Lyman-α forest
- significantly modifies late-time structure formation:
  - suppresses late dwarf formation (in accordance with SFHs): "missing satellites", void phenomenon, H I-mass function
  - group/cluster bimodality of core entropy values

When do clusters form?

mass accretion history

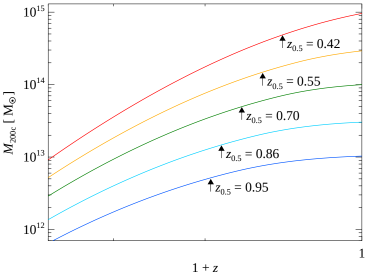

mass accretion rates

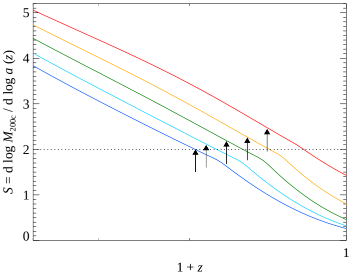

C.P., Chang, Broderick (2012)

- most cluster gas accretes after $z = 1$, when blazar heating can have a large effect (for late forming objects)!

Entropy floor in clusters

Cluster entropy profiles

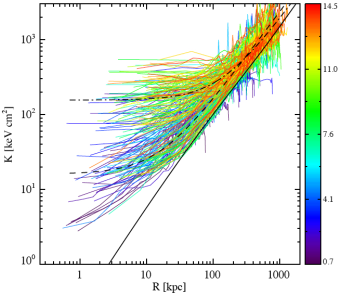

Cavagnolo+ (2009)

Planck stacking of optical clusters

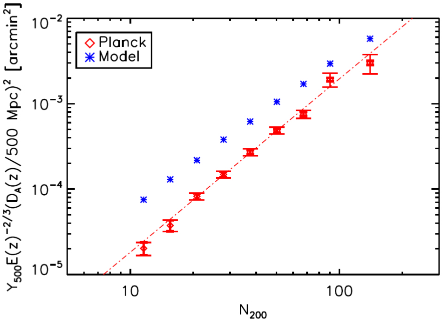

Planck Collaboration (2011)

- Do optical and X-ray/Sunyaev-Zel'dovich cluster observations probe the same population? (Hicks+ 2008, Planck Collaboration 2011)

Entropy profiles: effect of blazar heating

varying formation time

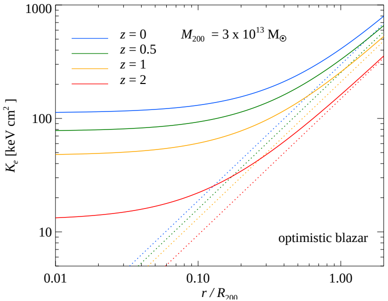

varying cluster mass

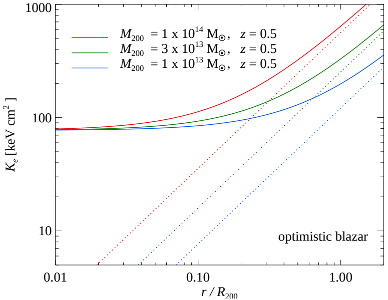

C.P., Chang, Broderick (2012)

assume big fraction of intra-cluster medium collapses from IGM:

- redshift-dependent entropy excess in cores
- greatest effect for late forming groups/small clusters

Gravitational reprocessing of entropy floors

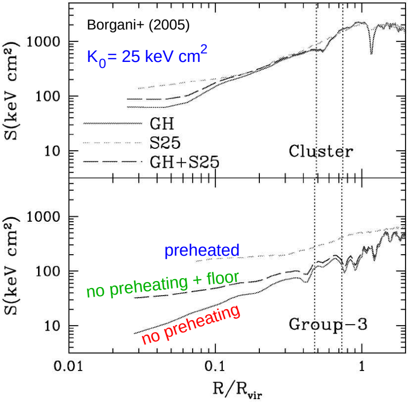

Borgani+ (2005)

- greater initial entropy K_0
  $\rightarrow$ more shock heating
  $\rightarrow$ greater increase in K_0
  over entropy floor
- net K_0 amplification of 3-5
- expect:

  median $K_{e,0} \sim 150\,\mathrm{keV\,cm}^2$

  max. $K_{e,0} \sim 600\,\mathrm{keV\,cm}^2$

Cool-core versus non-cool core clusters

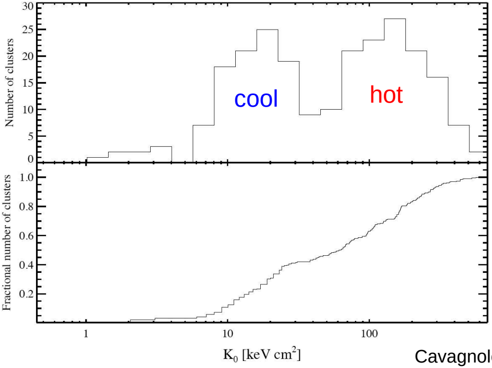

Cavagnolo+ (2009)

Cool-core versus non-cool core clusters

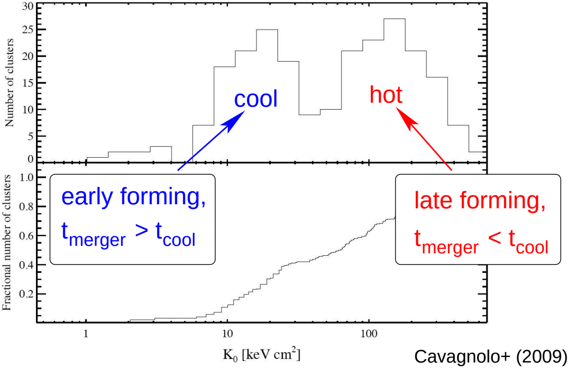

Cavagnolo+ (2009)

- time-dependent preheating + gravitational reprocessing $\longrightarrow$ CC-NCC bifurcation (two attractor solutions)
- need hydrodynamic simulations to confirm this scenario

How efficient is heating by AGN feedback?

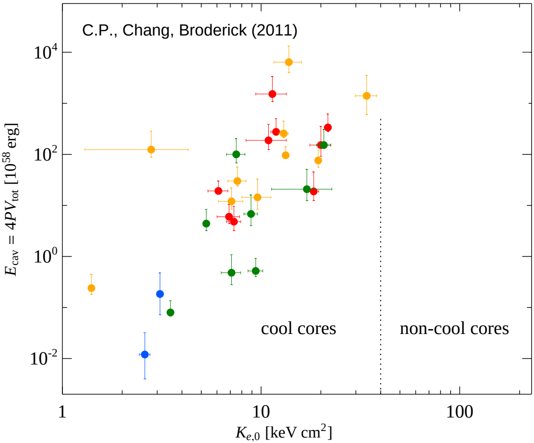

How efficient is heating by AGN feedback?

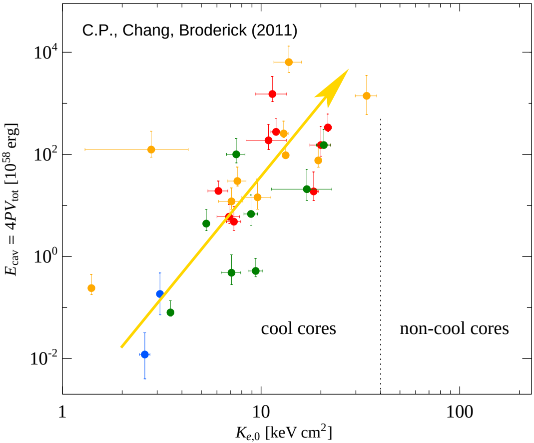

How efficient is heating by AGN feedback?

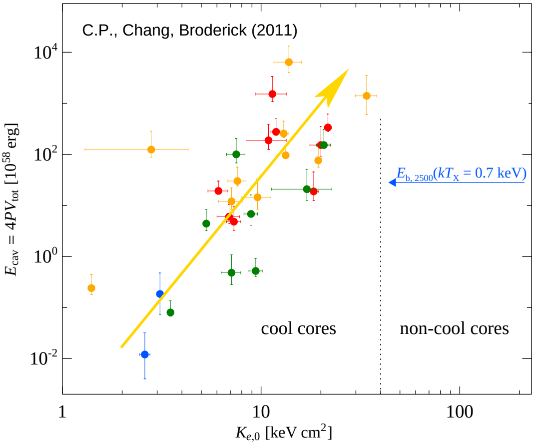

How efficient is heating by AGN feedback?

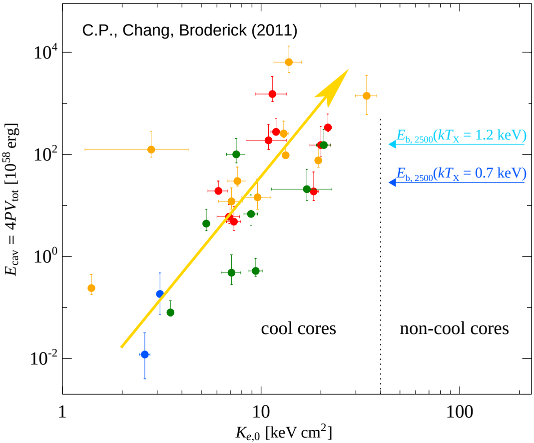

How efficient is heating by AGN feedback?

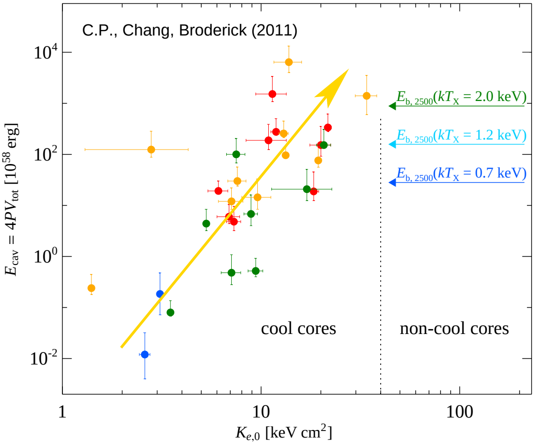

How efficient is heating by AGN feedback?

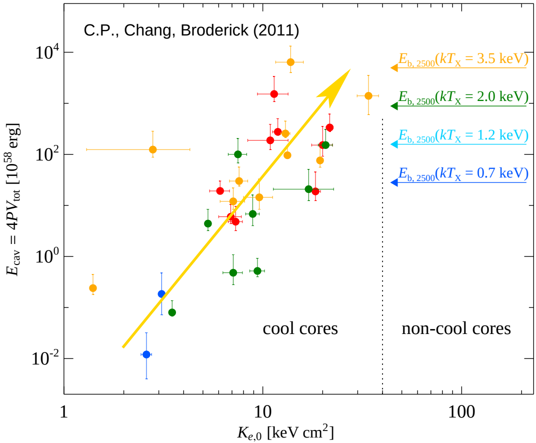

How efficient is heating by AGN feedback?

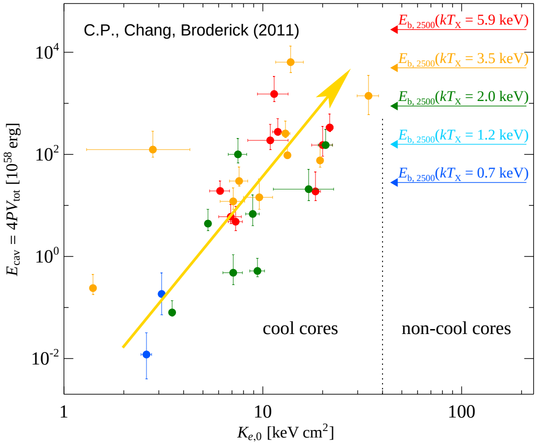

How efficient is heating by AGN feedback?

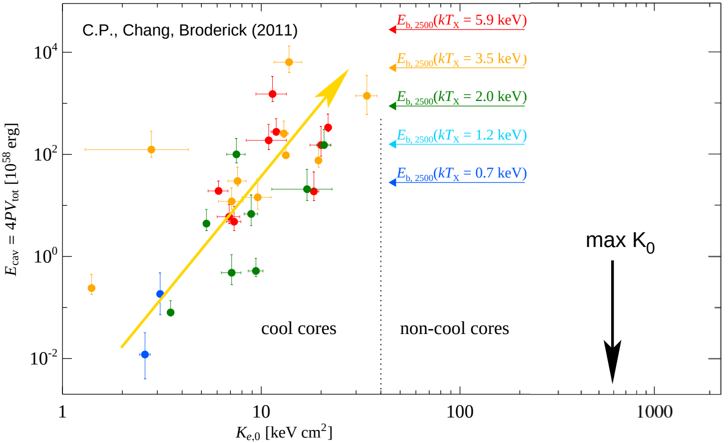

AGNs cannot transform CC to NCC clusters (on a buoyancy timescale)